Supplementary : data analysis methods

April 1, 2024

Contents

1 Quality control

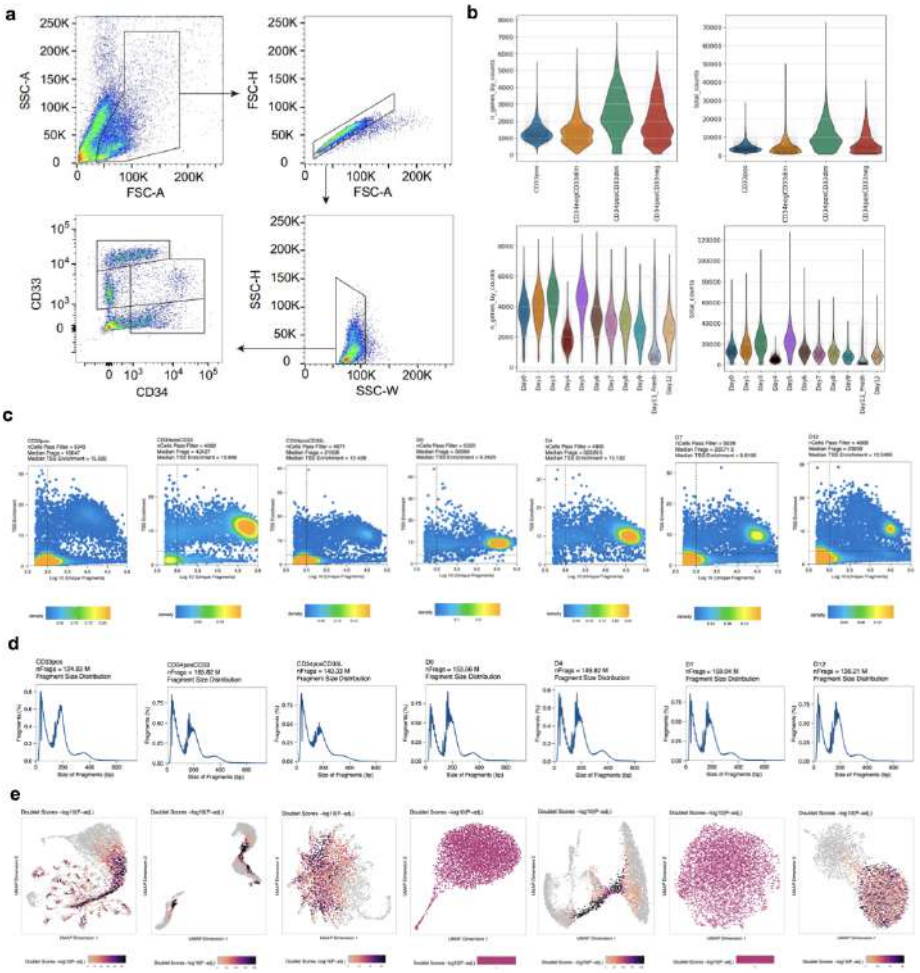

Figure 1: Supplementary: a. Gating strategy used for FACS sorting on human bone marrow cells. b. Quality control for RNA samples. Violin plots show the number of non-zero genes and total counts per cell for indifivudla samples (top for sorted samples, bottom for timepoints samples). c,d,e. Quality control for ATAC samples: TSS by unique fragments, fragment size distribution, doublet scores

2 Cell type annotation

2.1 Scatter plots

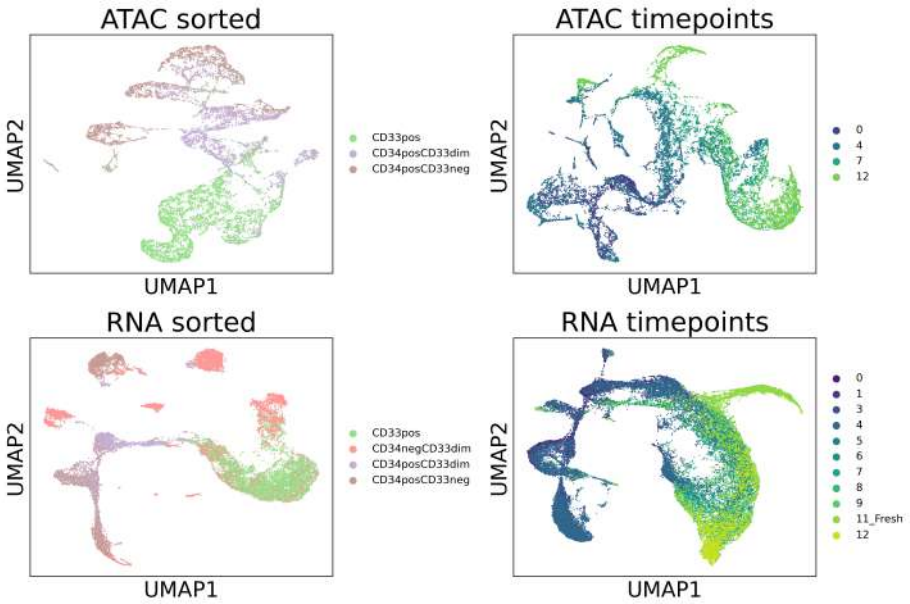

Figure 2: Supplementary: Time points (days) and sorted assays (CD) annotation

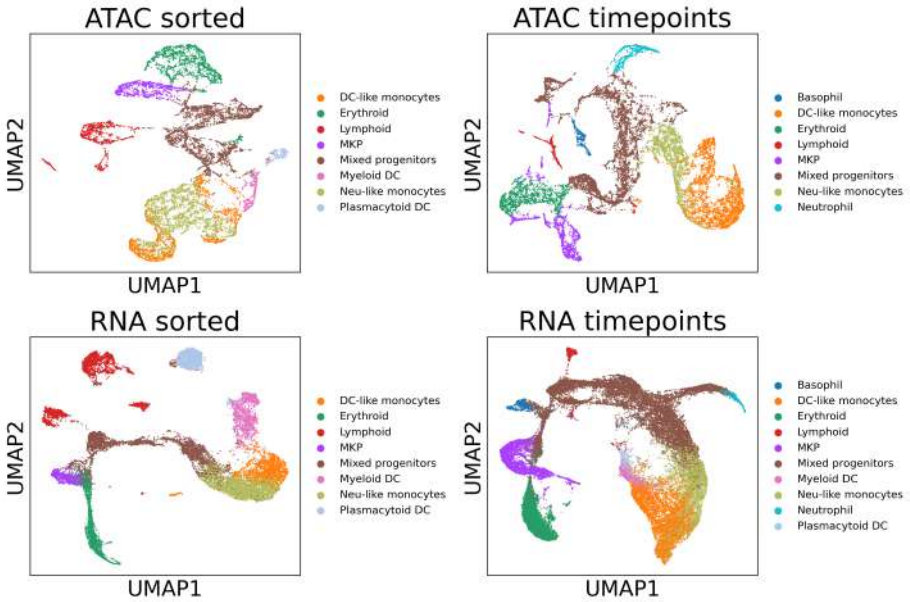

Figure 3: Supplementary: Leiden identity simple annotation

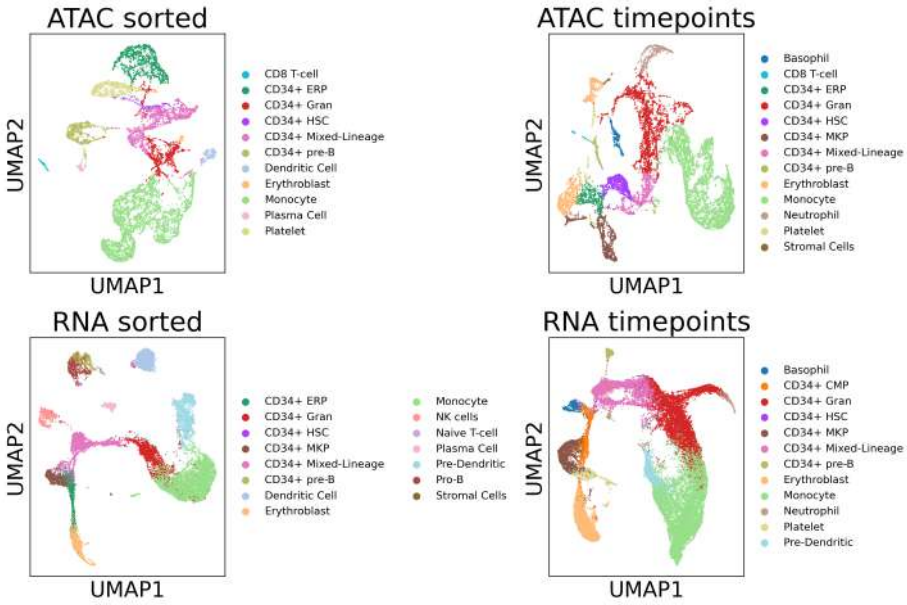

Figure 4: Supplementary: Leiden identity annotation

2.2 Bar plots

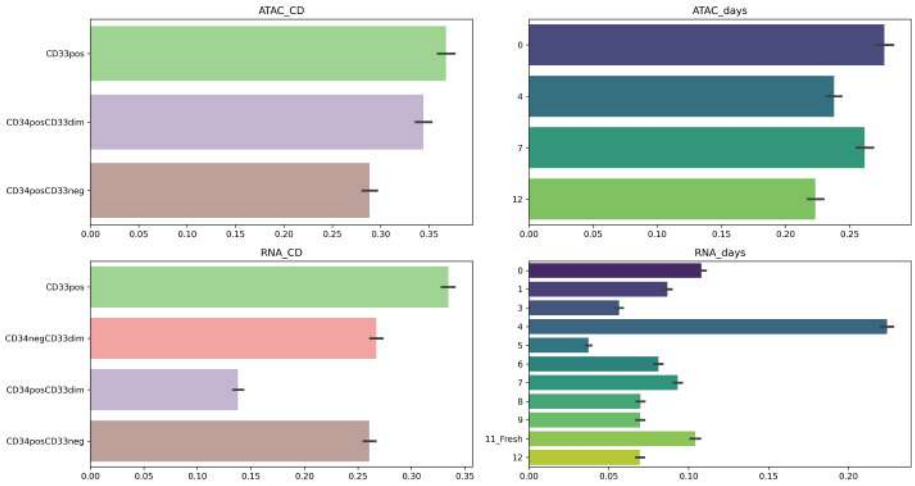

Figure 5: Supplementary: Leiden identity simple annotation

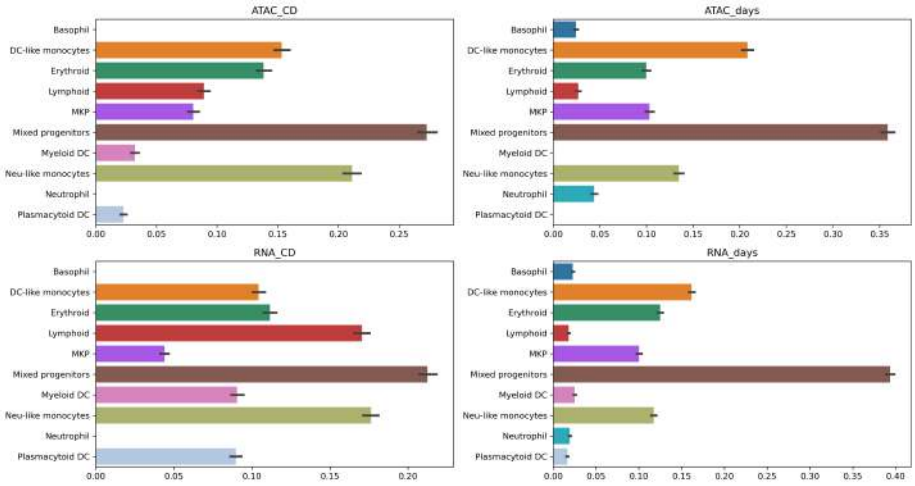

Figure 6: Supplementary: Leiden identity simple annotation

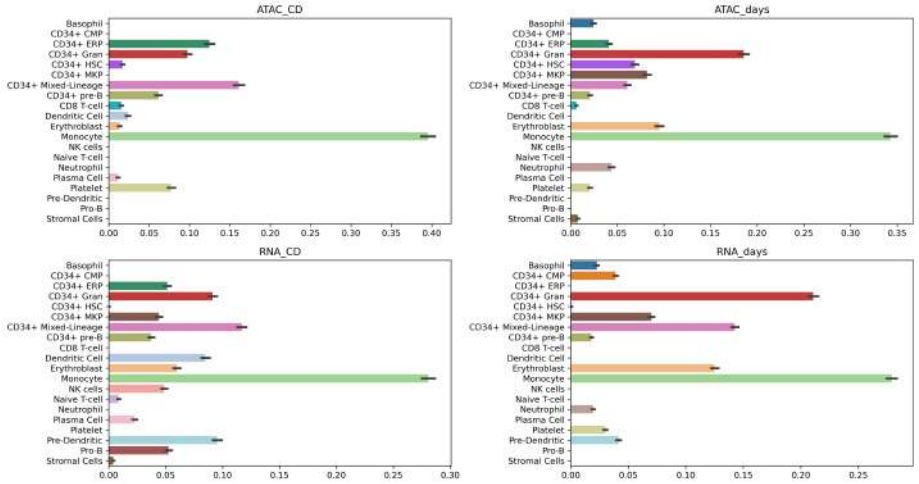

Figure 7: Supplementary: Leiden identity annotation

2.3 Correlation plots

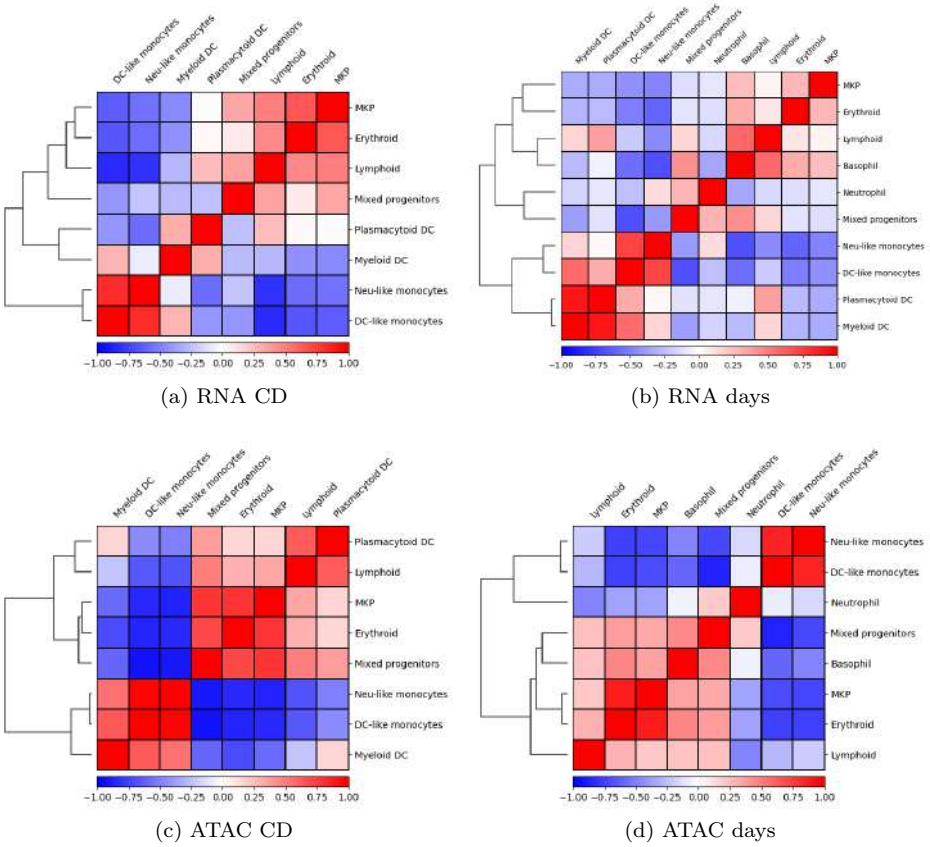

(a) RNA CD

(b) RNA days

(c) ATAC CD

(d) ATAC days

Figure 8: Correlation between cell type averages (obtained using top PCs)

3 Data integration

3.1 Linear optimal transport

3.1.1 Scatter plots

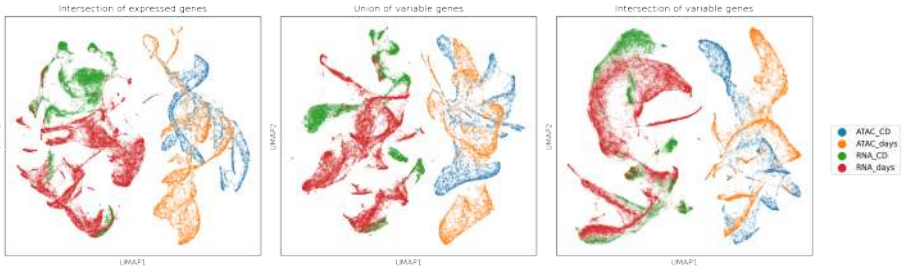

Figure 9: Assays in RNA days PCA subspace

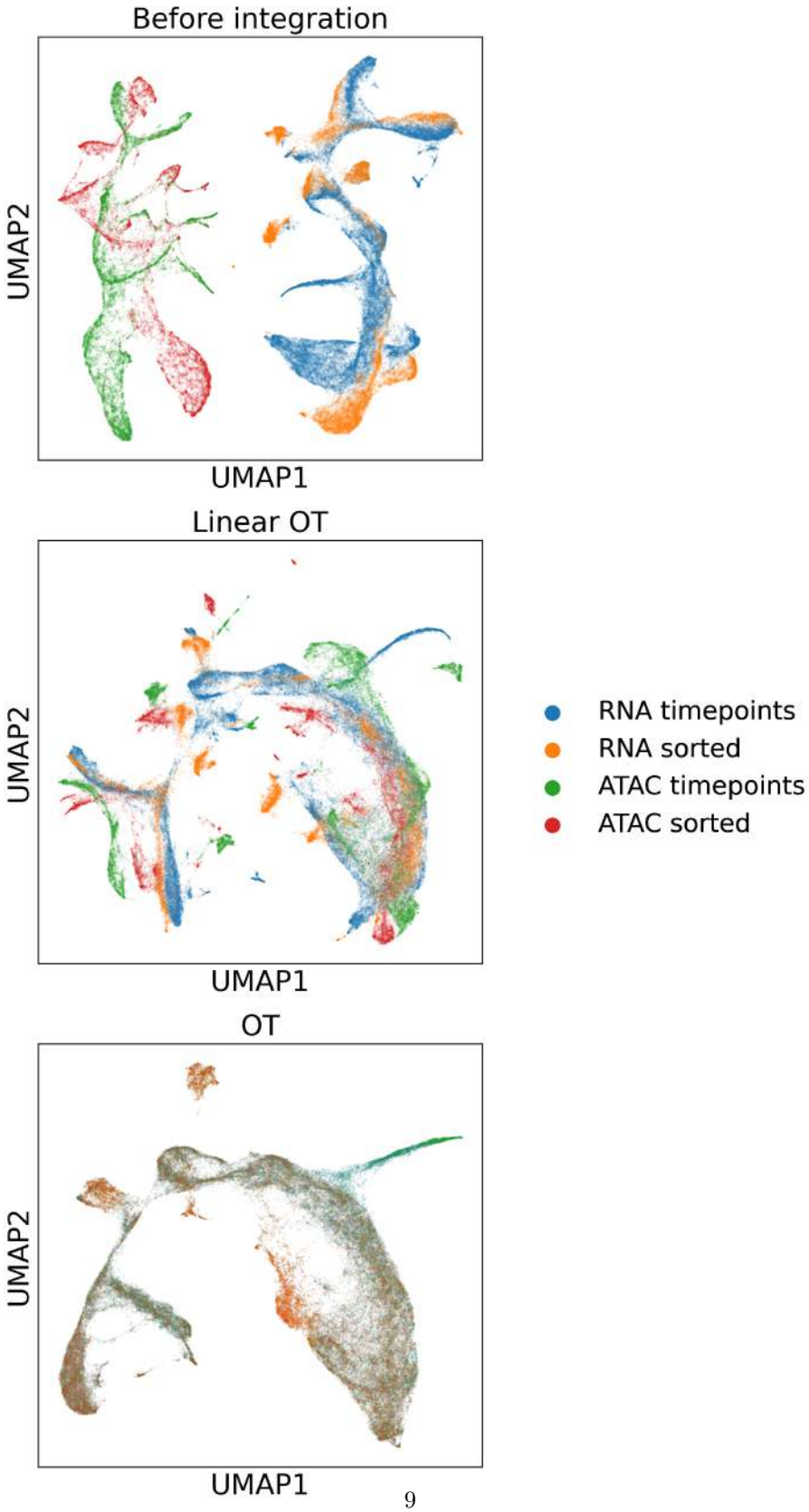

Figure 10: Assays in RNA days PCA subspace, after alignment with linear optimal transport

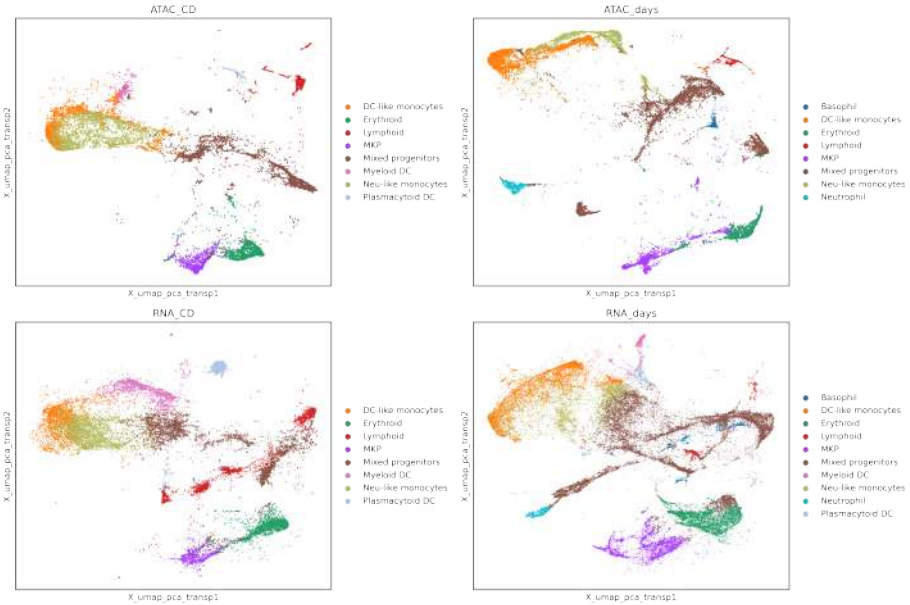

Figure 11: Assays in RNA days PCA subspace obtained using the intersection of expressed genes, after alignment with linear optimal transport.

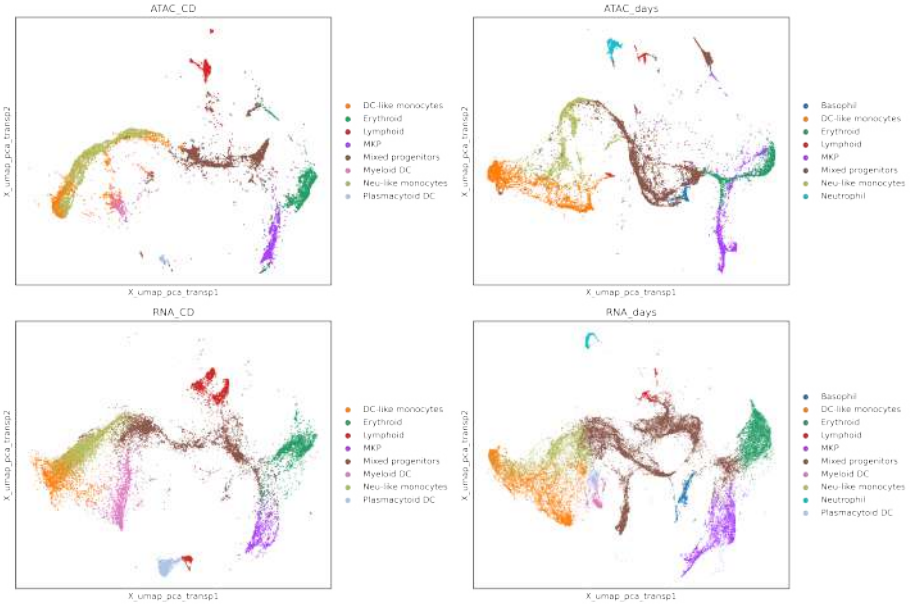

Figure 12: Assays in RNA days PCA subspace obtained using the union of variable genes, after alignment with linear optimal transport.

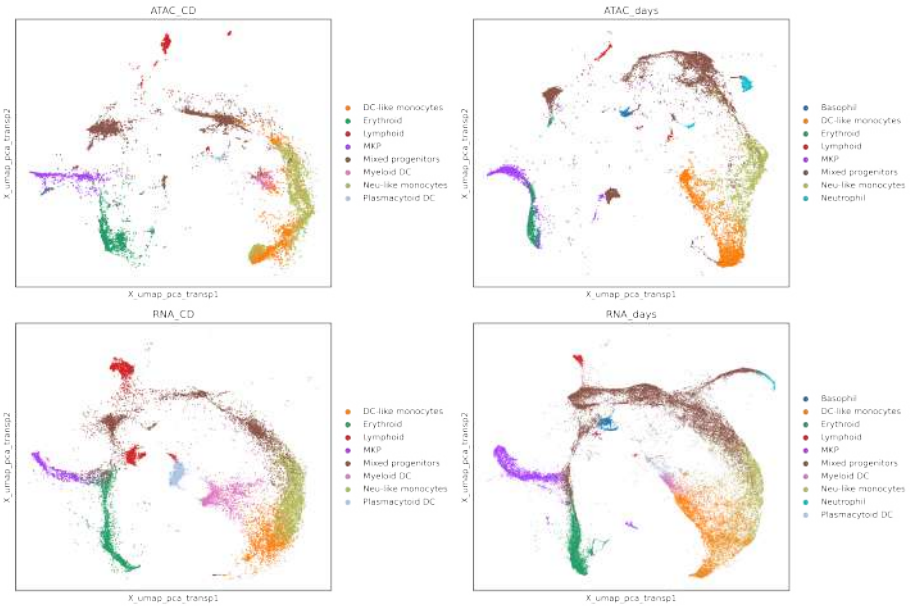

Figure 13: Assays in RNA days PCA subspace obtained using the intersection of variable genes, after alignment with linear optimal transport.

3.1.2 Correlation plots

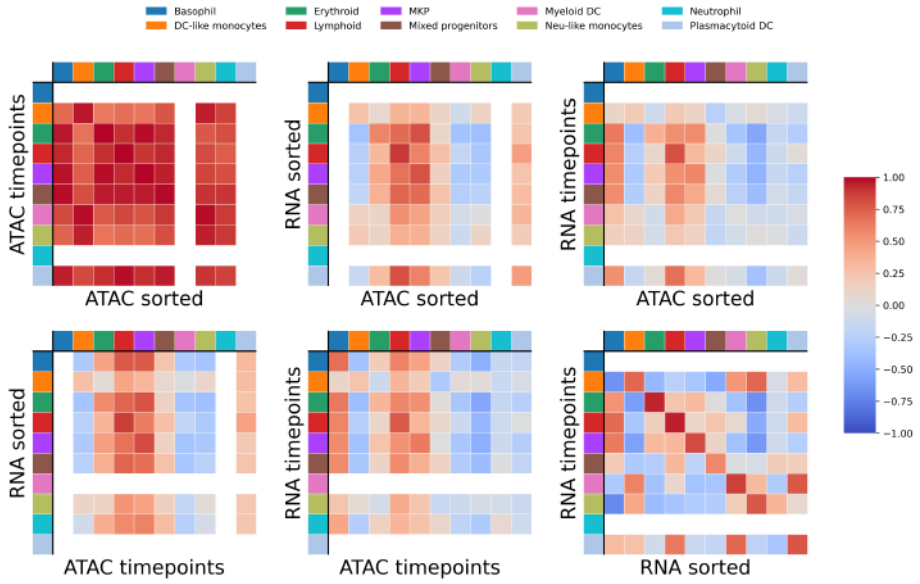

Figure 14: Correlation between assays' cell type averages (obtained using top PCs of assays, each in their own PCA subspace)

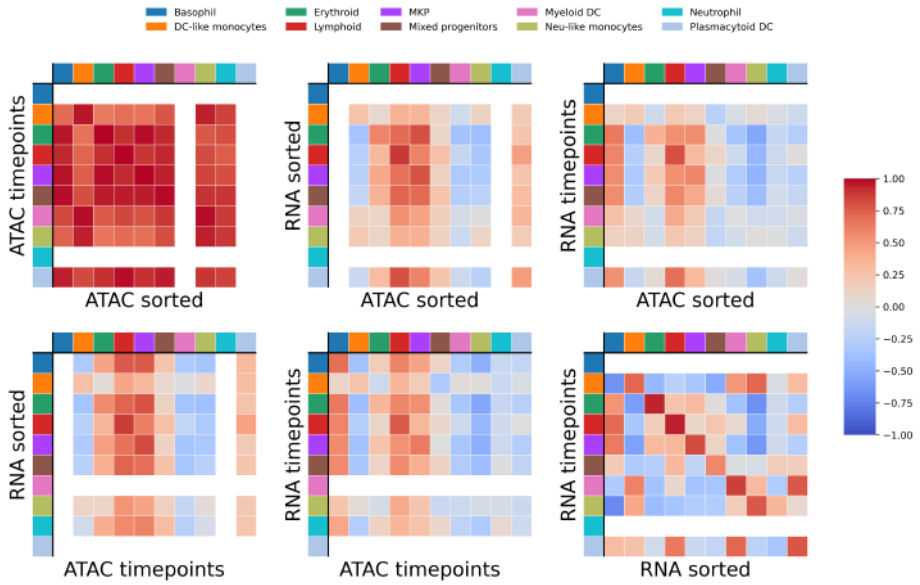

Figure 15: Correlation between assays' cell type averages (obtained using top PCs of assays in RNA days PCA subspace)

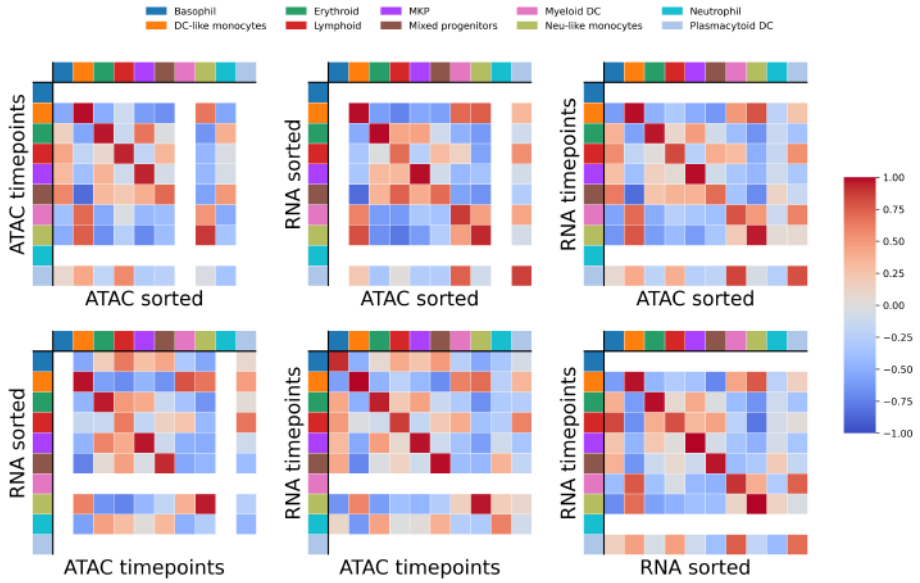

Figure 16: Correlation between assays' cell type averages (obtained using top PCs of assays in RNA days PCA subspace, after alignment with linear optimal transport)

3.2 Supervised optimal transport

Grouping of categories to go from full to simple annotation

- 'Early-ERP','Erythroblast','CD34+ ERP' = 'Erythroid'
- 'Platelet','CD34+ MKP' = 'MKP'
- 'Pre-Dendritic','Dendritic Cell' = 'Dendritic'
- 'CD34+ CLP','CD34+ pre-B','Pro-B','Plasma Cell', 'NK cells','Naive T-cell','CD8 T-cell' = 'Lymphoid'
- 'CD34+ Mixed-Lineage', 'CD34+ HSC','CD34+ CMP', 'CD34+ Gran', 'Eosinophil','Stromal Cells' = 'Mixed-Lineage'
- change unlikely 'Erythroid' annotation (outlier, mixed cluster) for late ATAC days (day 7 and 12) to 'Mixed-Lineage'

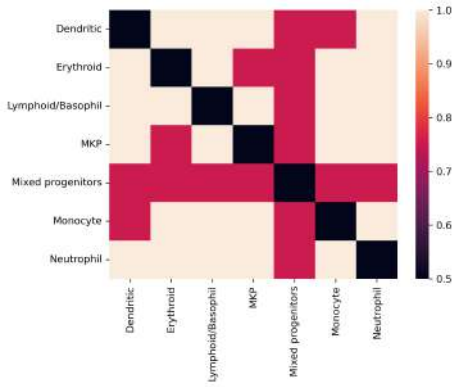

Figure 17: Supplementary: supervision of OT cost matrix

4 HSC score

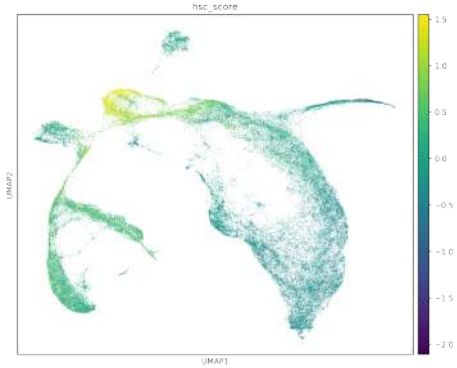

Figure 18: Supplementary: hematopoeitic stem cell score

5 Trajectory inference

5.1 Trajectory in PCA space

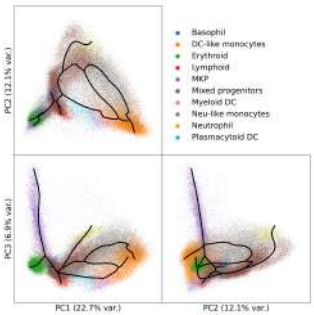

Figure 19: Supplementary: Trajectory visualized in PCA space

6 Trajectory analysis

6.1 Erythroid branch

6.1.1 Pseudotime

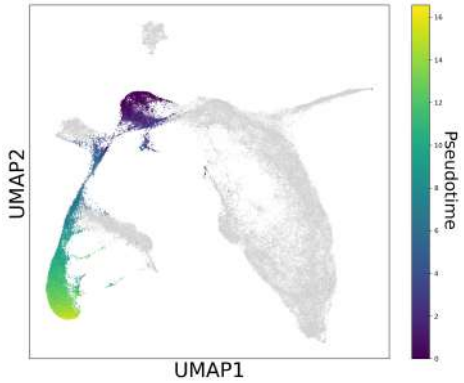

Figure 20: Supplementary: Erythroid branch pseudotime

6.1.2 Volcanos

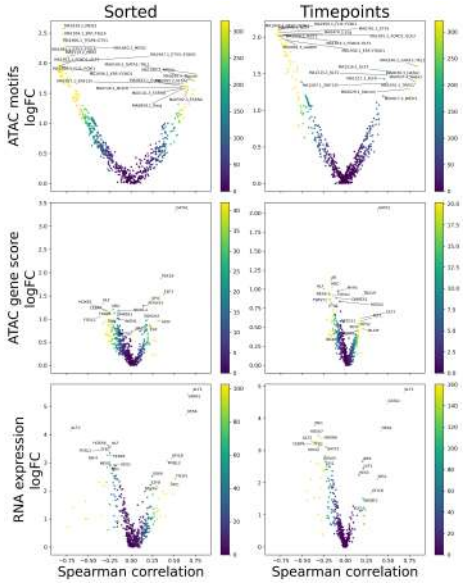

Figure 21: Supplementary: Erythroid branch marker detection with Spearman correlation. The volcano plot is colored by -log10 adjusted p-values

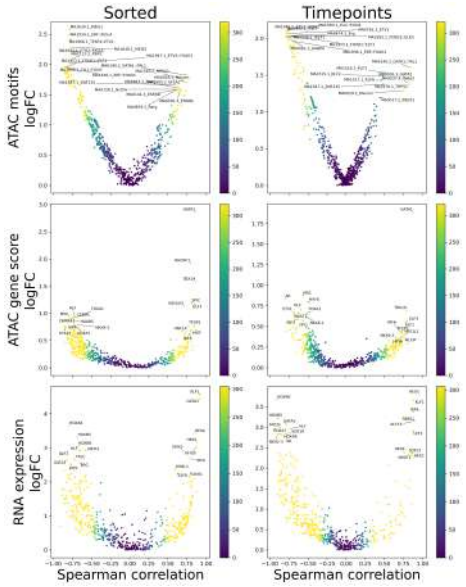

Figure 22: Supplementary: Erythroid branch marker detection with Spearman correlation and MAGIC imputed matrices for gene score and RNA expression. The volcano plot is colored by -log10 adjusted p-values

6.1.3 Heatmap

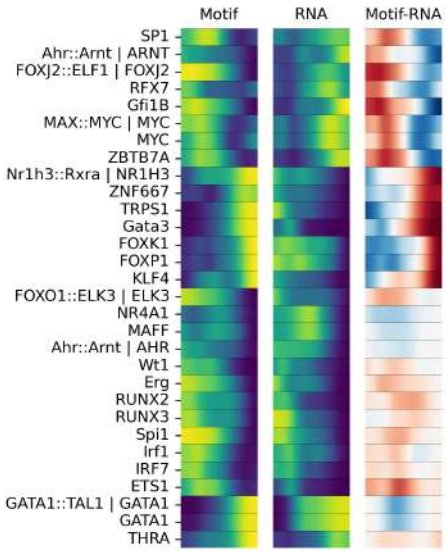

Figure 23: Supplementary: Heatmap of top negative and positive correlations against pseudotime, grouping all RNA and chromVAR assays

6.1.4 X plots

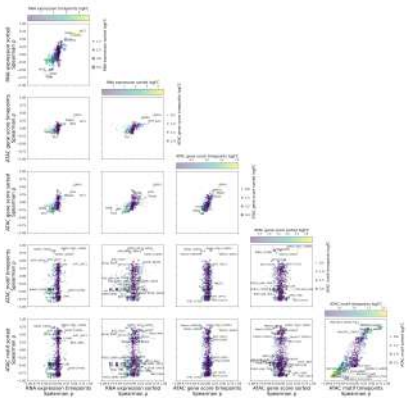

Figure 24: Supplementary: X-plot showing Spearman correlations against pseudotime, for all pairs of assays

6.2 MKP branch

6.2.1 Pseudotime

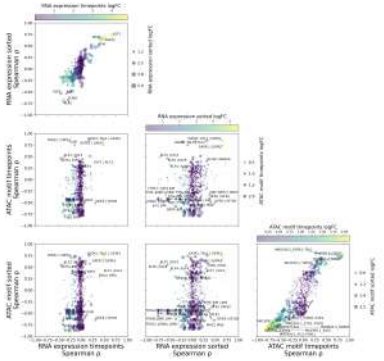

Figure 25: Supplementary: X-plot showing Spearman correlations against pseudotime, grouping sorted and timepoints assays for RNA and gene score

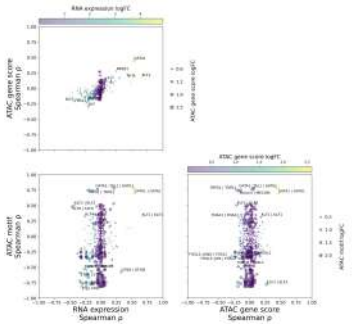

Figure 26: Supplementary: X-plot showing Spearman correlations against pseudotime, grouping all RNA and chromVAR assays

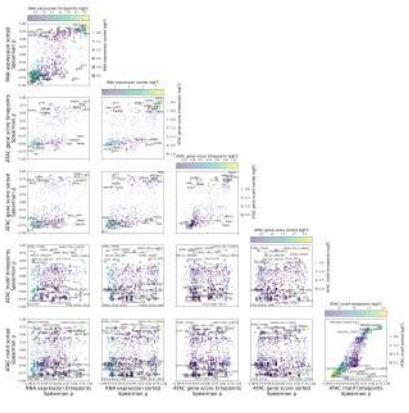

Figure 27: Supplementary: X-plot showing Spearman correlations against pseudotime, for all pairs of assays, with MAGIC smoothing for gene score and RNA expression

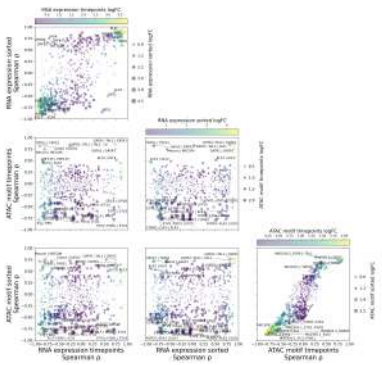

Figure 28: Supplementary: X-plot showing Spearman correlations against pseudotime, grouping sorted and timepoints assays for RNA and gene score, with MAGIC smoothing for gene score and RNA expression

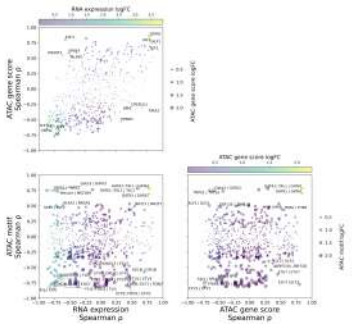

Figure 29: Supplementary: X-plot showing Spearman correlations against pseudotime, grouping all RNA and chromVAR assays with MAGIC smoothing for gene score and RNA expression

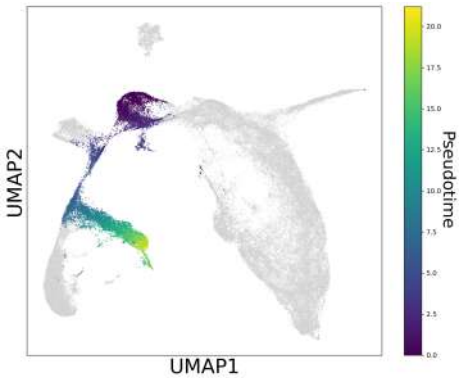

Figure 30: Supplementary: MKP branch pseudotime

6.2.2 Volcanos

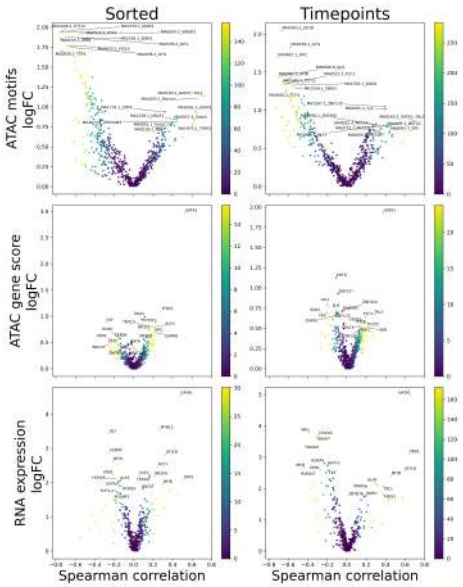

Figure 31: Supplementary: Erythroid branch marker detection with Spearman correlation. The volcano plot is colored by -log10 adjusted p-values

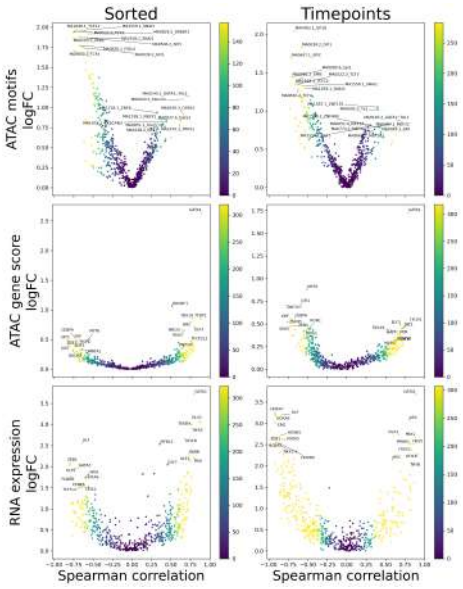

Figure 32: Supplementary: Erythroid branch marker detection with Spearman correlation and MAGIC imputed matrices for gene score and RNA expression. The volcano plot is colored by -log10 adjusted p-values

6.2.3 Heatmap

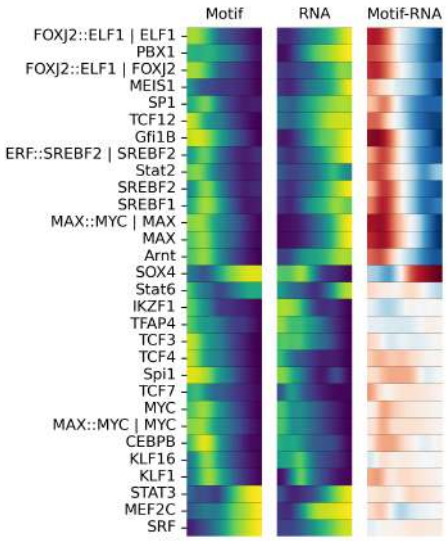

Figure 33: Supplementary: Heatmap of top negative and positive correlations against pseudotime, grouping all RNA and chromVAR assays

6.2.4 X plots

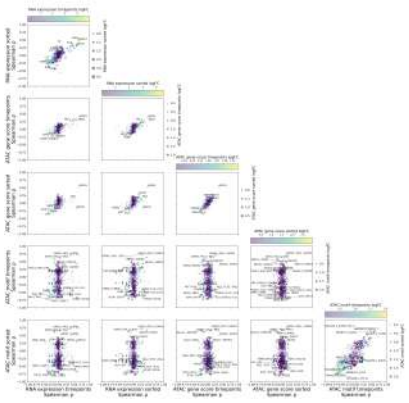

Figure 34: Supplementary: X-plot showing Spearman correlations against pseudotime, for all pairs of assays

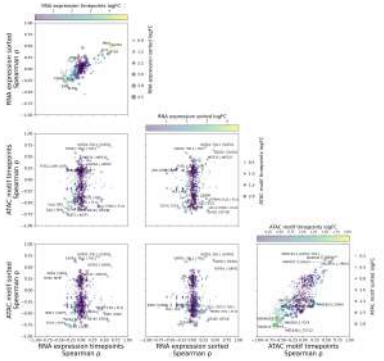

Figure 35: Supplementary: X-plot showing Spearman correlations against pseudotime, grouping sorted and timepoints assays for RNA and gene score

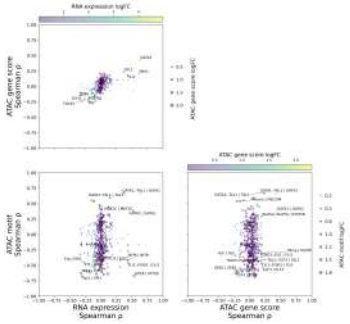

Figure 36: Supplementary: X-plot showing Spearman correlations against pseudotime, grouping all RNA and chromVAR assays

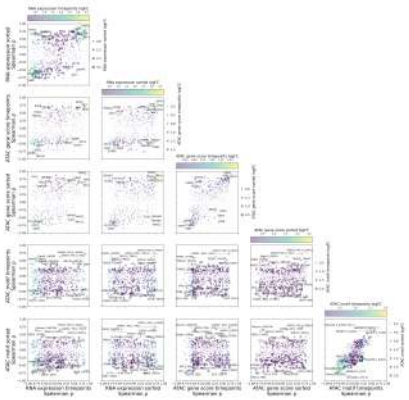

Figure 37: Supplementary: X-plot showing Spearman correlations against pseudotime, for all pairs of assays, with MAGIC smoothing for gene score and RNA expression

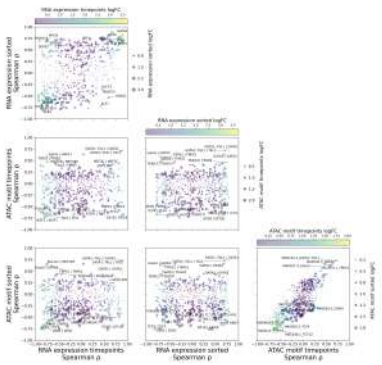

Figure 38: Supplementary: X-plot showing Spearman correlations against pseudotime, grouping sorted and timepoints assays for RNA and gene score, with MAGIC smoothing for gene score and RNA expression

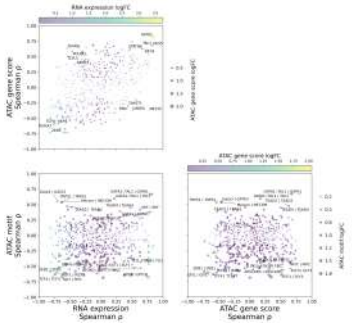

Figure 39: Supplementary: X-plot showing Spearman correlations against pseudotime, grouping all RNA and chromVAR assays with MAGIC smoothing for gene score and RNA expression

6.3 Basophil branch

6.3.1 Pseudotime

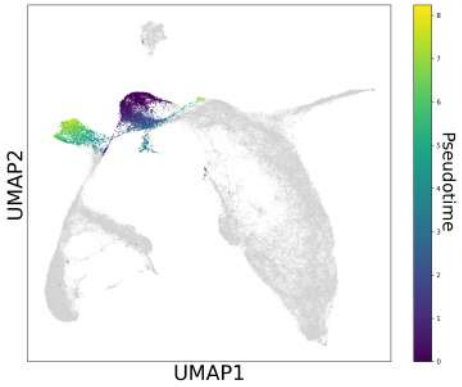

Figure 40: Supplementary: MKP branch pseudotime

6.3.2 Volcanos

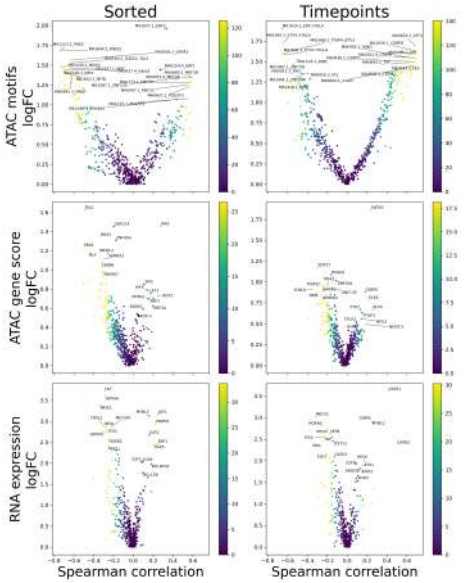

Figure 41: Supplementary: Erythroid branch marker detection with Spearman correlation. The volcano plot is colored by -log10 adjusted p-values

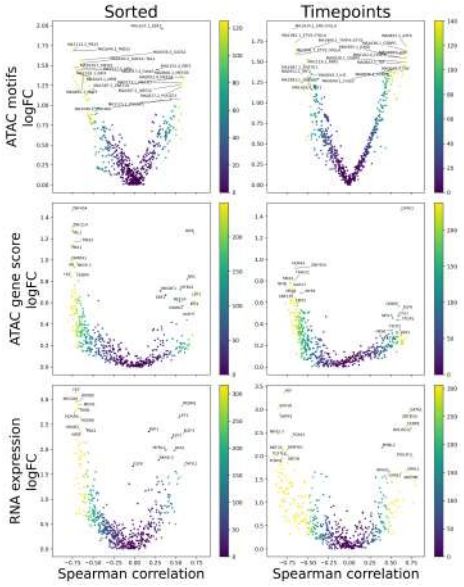

Figure 42: Supplementary: Erythroid branch marker detection with Spearman correlation and MAGIC imputed matrices for gene score and RNA expression. The volcano plot is colored by -log10 adjusted p-values

6.3.3 Heatmap

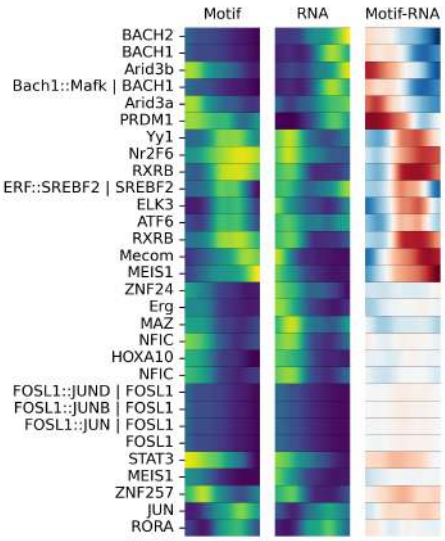

Figure 43: Supplementary: Heatmap of top negative and positive correlations against pseudotime, grouping all RNA and chromVAR assays

6.3.4 X plots

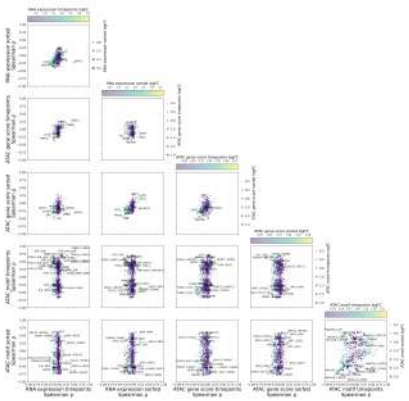

Figure 44: Supplementary: X-plot showing Spearman correlations against pseudotime, for all pairs of assays

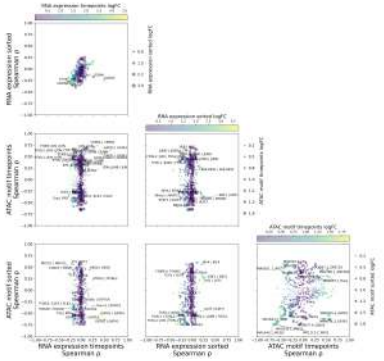

Figure 45: Supplementary: X-plot showing Spearman correlations against pseudotime, grouping sorted and timepoints assays for RNA and gene score

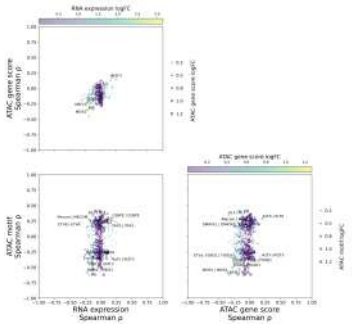

Figure 46: Supplementary: X-plot showing Spearman correlations against pseudotime, grouping all RNA and chromVAR assays

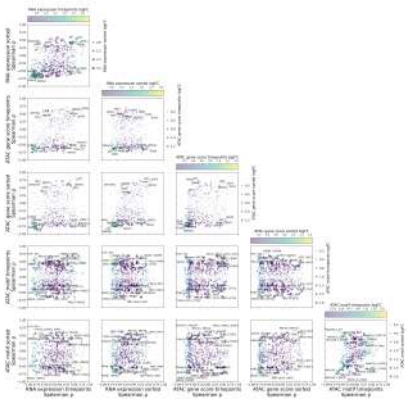

Figure 47: Supplementary: X-plot showing Spearman correlations against pseudotime, for all pairs of assays, with MAGIC smoothing for gene score and RNA expression

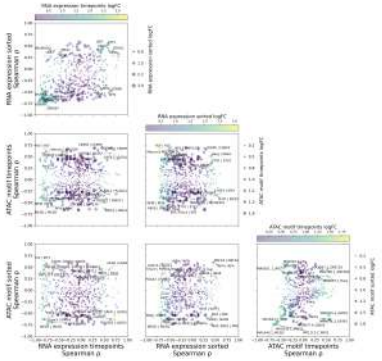

Figure 48: Supplementary: X-plot showing Spearman correlations against pseudotime, grouping sorted and timepoints assays for RNA and gene score, with MAGIC smoothing for gene score and RNA expression

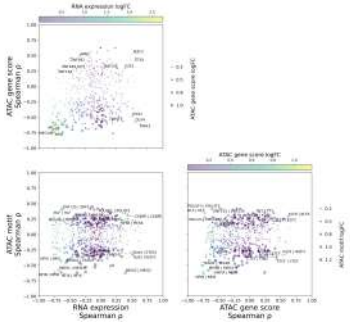

Figure 49: Supplementary: X-plot showing Spearman correlations against pseudotime, grouping all RNA and chromVAR assays with MAGIC smoothing for gene score and RNA expression

6.4 Neutrophil branch

6.4.1 Pseudotime

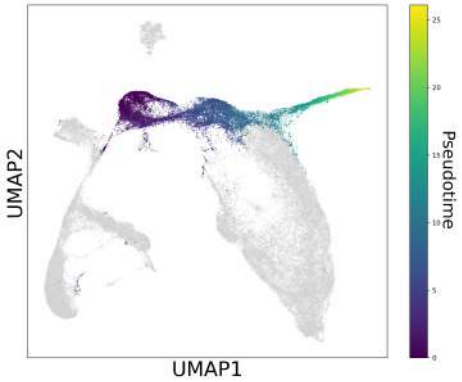

Figure 50: Supplementary: MKP branch pseudotime

6.4.2 Volcanos

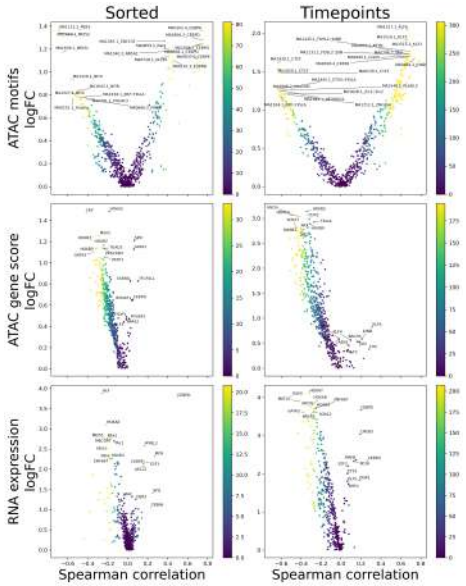

Figure 51: Supplementary: Erythroid branch marker detection with Spearman correlation. The volcano plot is colored by -log10 adjusted p-values

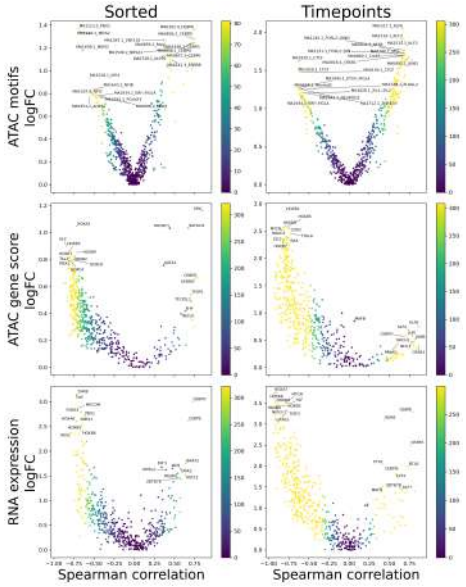

Figure 52: Supplementary: Erythroid branch marker detection with Spearman correlation and MAGIC imputed matrices for gene score and RNA expression. The volcano plot is colored by -log10 adjusted p-values

6.4.3 Heatmap

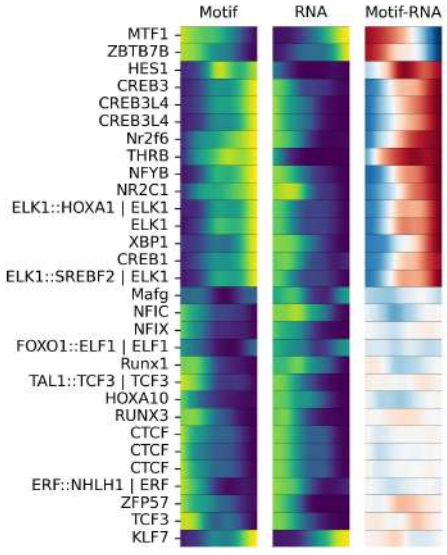

Figure 53: Supplementary: Heatmap of top negative and positive correlations against pseudotime, grouping all RNA and chromVAR assays

6.4.4 X plots

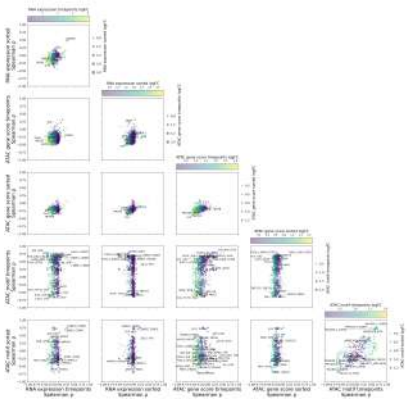

Figure 54: Supplementary: X-plot showing Spearman correlations against pseudotime, for all pairs of assays

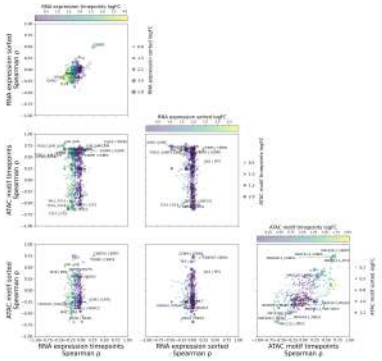

Figure 55: Supplementary: X-plot showing Spearman correlations against pseudotime, grouping sorted and timepoints assays for RNA and gene score

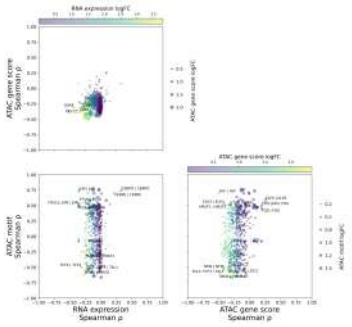

Figure 56: Supplementary: X-plot showing Spearman correlations against pseudotime, grouping all RNA and chromVAR assays

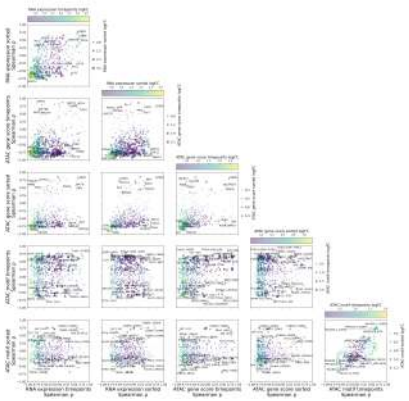

Figure 57: Supplementary: X-plot showing Spearman correlations against pseudotime, for all pairs of assays, with MAGIC smoothing for gene score and RNA expression

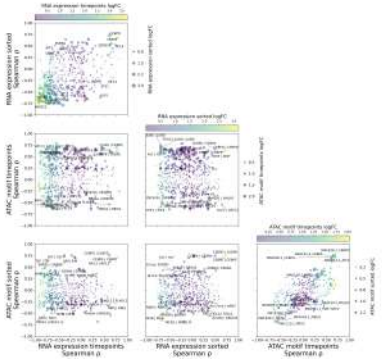

Figure 58: Supplementary: X-plot showing Spearman correlations against pseudotime, grouping sorted and timepoints assays for RNA and gene score, with MAGIC smoothing for gene score and RNA expression

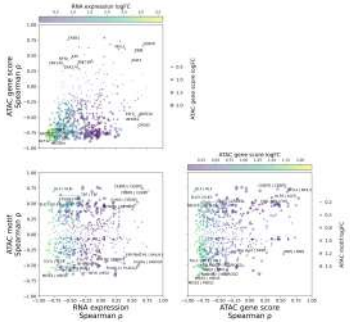

Figure 59: Supplementary: X-plot showing Spearman correlations against pseudotime, grouping all RNA and chromVAR assays with MAGIC smoothing for gene score and RNA expression

6.5 Monocyte branch

6.5.1 Pseudotime

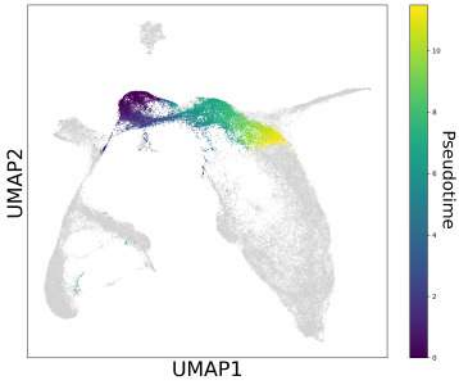

Figure 60: Supplementary: MKP branch pseudotime

6.5.2 Volcanos

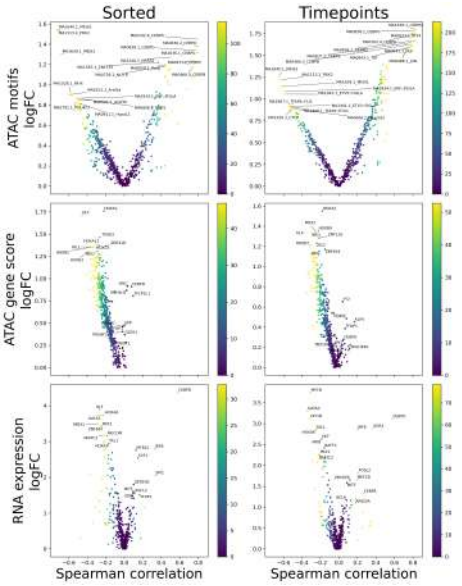

Figure 61: Supplementary: Erythroid branch marker detection with Spearman correlation. The volcano plot is colored by -log10 adjusted p-values

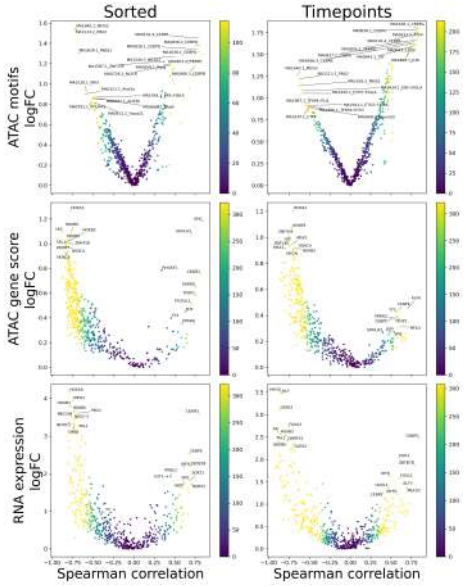

Figure 62: Supplementary: Erythroid branch marker detection with Spearman correlation and MAGIC imputed matrices for gene score and RNA expression. The volcano plot is colored by -log10 adjusted p-values

6.5.3 Heatmap

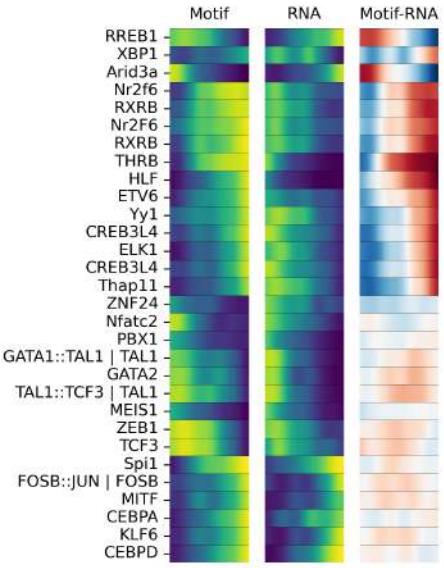

Figure 63: Supplementary: Heatmap of top negative and positive correlations against pseudotime, grouping all RNA and chromVAR assays

6.5.4 X plots

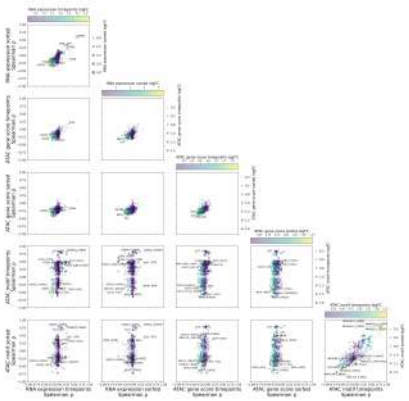

Figure 64: Supplementary: X-plot showing Spearman correlations against pseudotime, for all pairs of assays

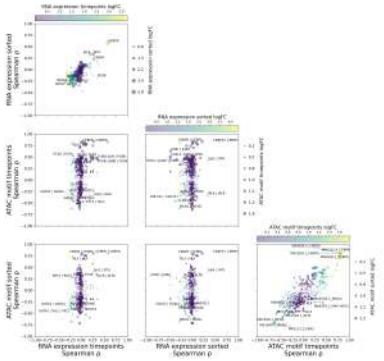

Figure 65: Supplementary: X-plot showing Spearman correlations against pseudotime, grouping sorted and timepoints assays for RNA and gene score

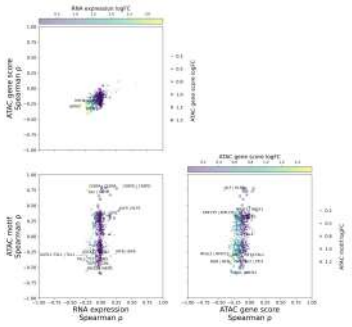

Figure 66: Supplementary: X-plot showing Spearman correlations against pseudotime, grouping all RNA and chromVAR assays

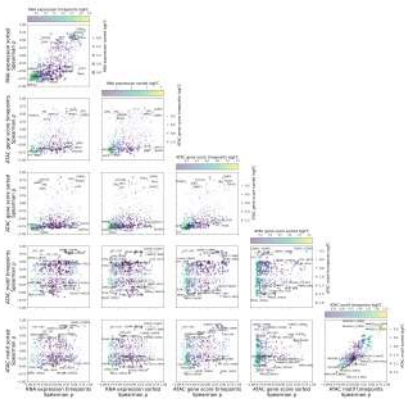

Figure 67: Supplementary: X-plot showing Spearman correlations against pseudotime, for all pairs of assays, with MAGIC smoothing for gene score and RNA expression

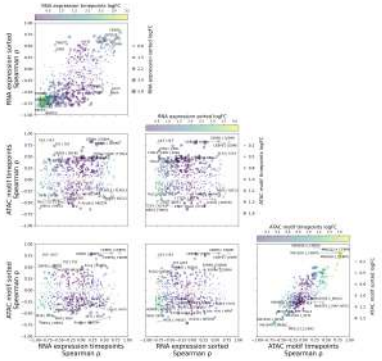

Figure 68: Supplementary: X-plot showing Spearman correlations against pseudotime, grouping sorted and timepoints assays for RNA and gene score, with MAGIC smoothing for gene score and RNA expression

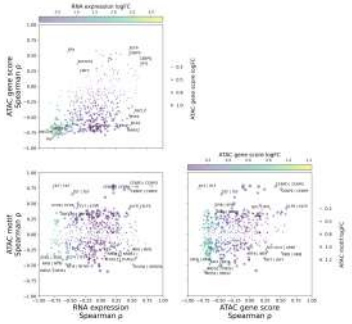

Figure 69: Supplementary: X-plot showing Spearman correlations against pseudotime, grouping all RNA and chromVAR assays with MAGIC smoothing for gene score and RNA expression

6.6 Myeloid DC branch

6.6.1 Pseudotime

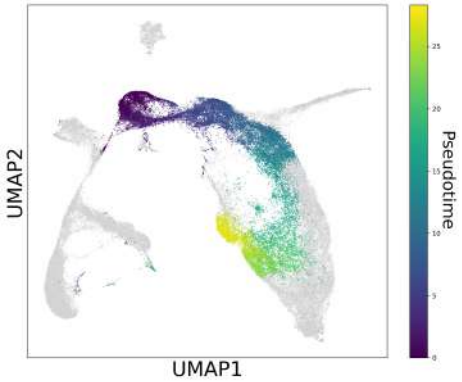

Figure 70: Supplementary: MKP branch pseudotime

6.6.2 Volcanos

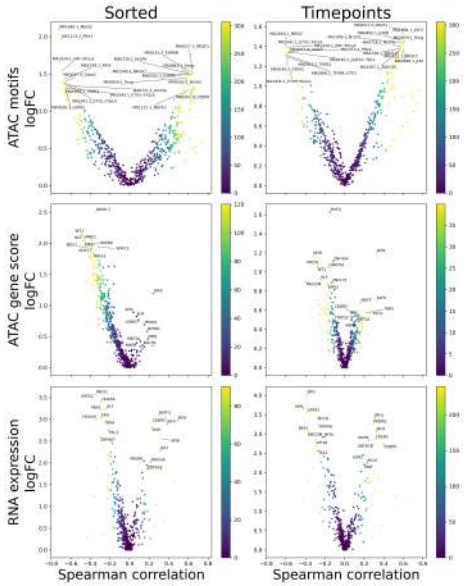

Figure 71: Supplementary: Erythroid branch marker detection with Spearman correlation. The volcano plot is colored by -log10 adjusted p-values

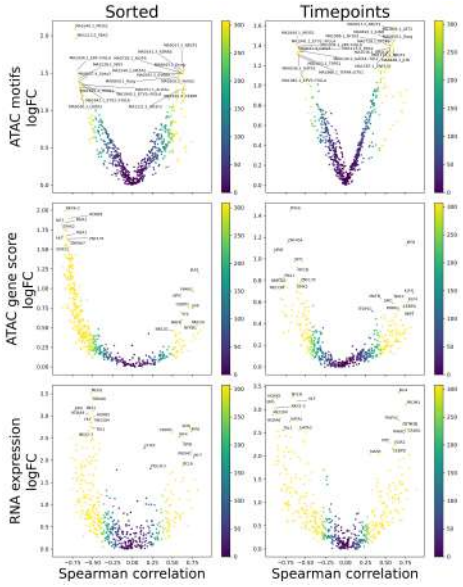

Figure 72: Supplementary: Erythroid branch marker detection with Spearman correlation and MAGIC imputed matrices for gene score and RNA expression. The volcano plot is colored by -log10 adjusted p-values

6.6.3 Heatmap

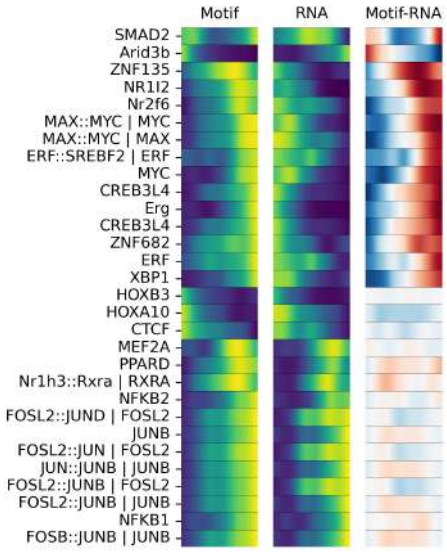

Figure 73: Supplementary: Heatmap of top negative and positive correlations against pseudotime, grouping all RNA and chromVAR assays

6.6.4 X plots

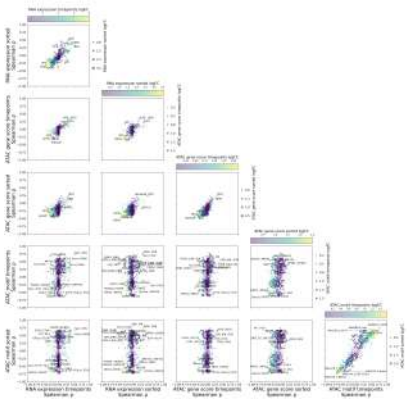

Figure 74: Supplementary: X-plot showing Spearman correlations against pseudotime, for all pairs of assays

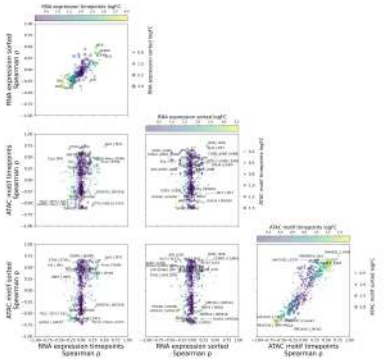

Figure 75: Supplementary: X-plot showing Spearman correlations against pseudotime, grouping sorted and timepoints assays for RNA and gene score

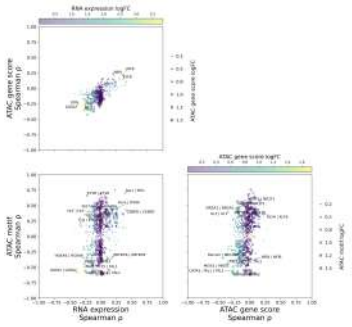

Figure 76: Supplementary: X-plot showing Spearman correlations against pseudotime, grouping all RNA and chromVAR assays

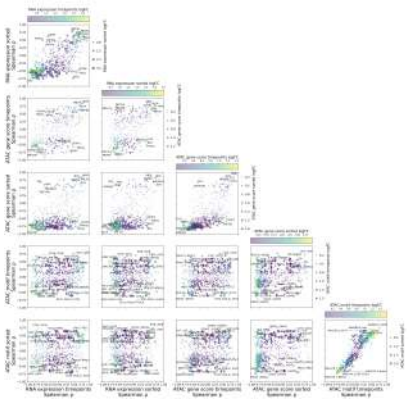

Figure 77: Supplementary: X-plot showing Spearman correlations against pseudotime, for all pairs of assays, with MAGIC smoothing for gene score and RNA expression

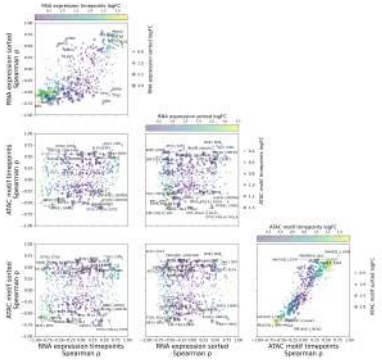

Figure 78: Supplementary: X-plot showing Spearman correlations against pseudotime, grouping sorted and timepoints assays for RNA and gene score, with MAGIC smoothing for gene score and RNA expression

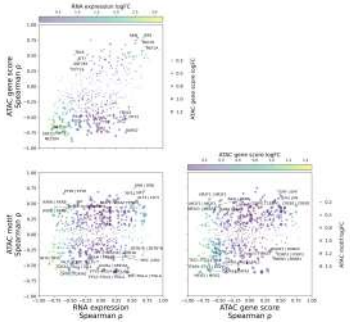

Figure 79: Supplementary: X-plot showing Spearman correlations against pseudotime, grouping all RNA and chromVAR assays with MAGIC smoothing for gene score and RNA expression

7 Early populations

7.1 Top markers from lineage tracing

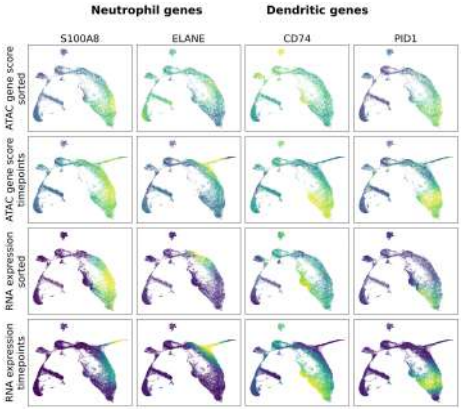

Figure 80: Supplementary: Marker genes previously identified by lineage tracing distinguish early monocyte populations: dendritic-like and neutrophil-like

7.2 Early populations classification by backpropagating labels

7.2.1 UMAP

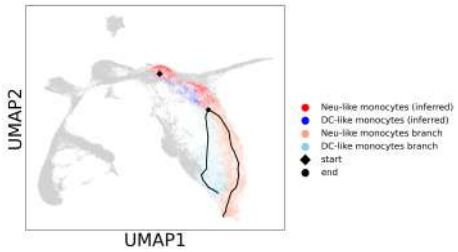

Figure 81: Supplementary: UMAP showing inferred dendritic-like and neutrophil-like early monocyte populations

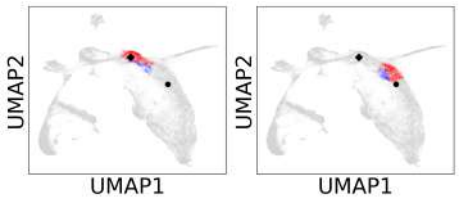

Figure 82: Supplementary: UMAP showing inferred dendritic-like and neutrophil-like early monocyte populations, split into "early" and "late" halves of pseudotime.

7.2.2 Volcanos

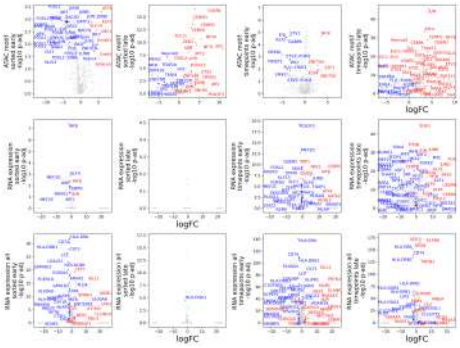

Figure 83: Supplementary: Volcano plots of Wilcoxon test between inferred dendritic-like and neutrophil-like early monocyte populations, for "early" and "late" halves of pseudotime. Motifs and RNA expression show TFs only while RNA expression all shows all genes

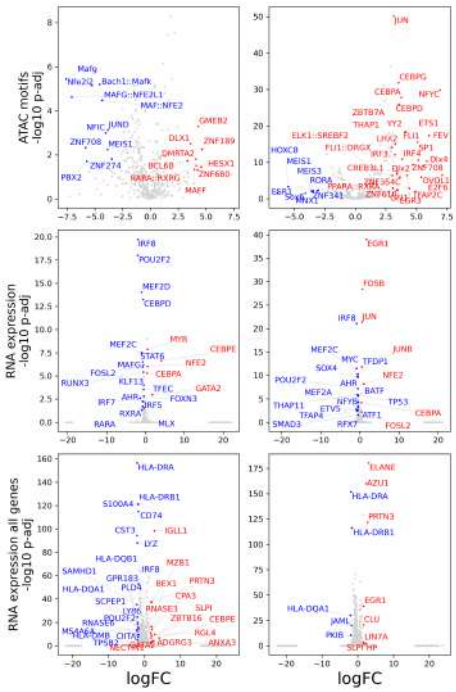

Figure 84: Supplementary: Volcano plots of Wilcoxon test between inferred dendritic-like and neutrophil-like early monocyte populations, for "early" and "late" halves of pseudotime, grouping assays. Motifs and RNA expression show TFs only while RNA expression all shows all genes

7.3 Early populations classification using known lineage tracing markers

7.3.1 UMAP

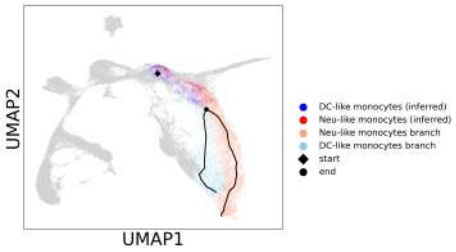

Figure 85: Supplementary: UMAP showing inferred dendritic-like and neutrophil-like early monocyte populations

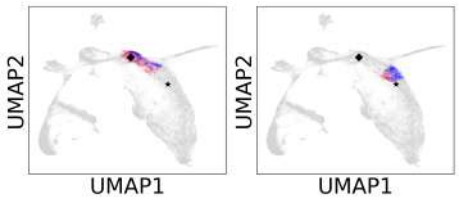

Figure 86: Supplementary: UMAP showing inferred dendritic-like and neutrophil-like early monocyte populations, split into "early" and "late" halves of pseudotime.

7.3.2 Volcanos

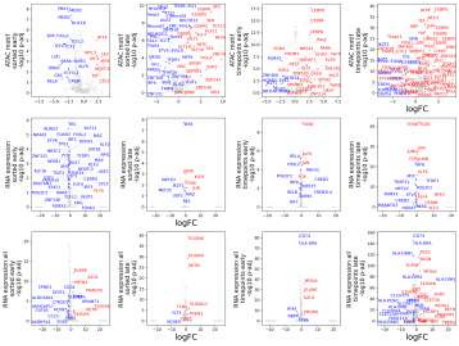

Figure 87: Supplementary: Volcano plots of Wilcoxon test between inferred dendritic-like and neutrophil-like early monocyte populations, for "early" and "late" halves of pseudotime. Motifs and RNA expression show TFs only while RNA expression all shows all genes